General Disclaimer

One or more of the Following Statements may affect this Document

- This document has been reproduced from the best copy furnished by the organizational source. It is being released in the interest of making available as much information as possible.

- This document may contain data, which exceeds the sheet parameters. It was furnished in this condition by the organizational source and is the best copy available.

- This document may contain tone-on-tone or color graphs, charts and/or pictures, which have been reproduced in black and white.

- This document is paginated as submitted by the original source.

- Portions of this document are not fully legible due to the historical nature of some of the material. However, it is the best reproduction available from the original submission.

Produced by the NASA Center for Aerospace Information (CASI)

GEOLOGICAL MAPPING IN NORTHWESTERN SAUDI ARABIA USING LANDSAT-MULTISPECTRAL TECHNIQUES

H. W. BLODGET
G. F. BROWN
J. G. MOIK

AUGUST 1975

GODDARD SPACE FLIGHT CENTER
GREENBELT, MARYLAND

GEOLOGICAL MAPPING IN NORTHWESTERN SAUDI ARABIA

USING LANDSAT-MULTISPECTRAL TECHNIQUES

H. W. Blodget
NASA Goddard Space Flight Center, Greenbelt, Md.

G. F. Brown
U.S. Geological Survey, Reston, Va.

J. G. Moik
Computer Sciences Corp., Silver Spring, Md.

August 1975

GODDARD SPACE FLIGHT CENTER
Greenbelt, Maryland

GEOLOGICAL MAPPING IN NORTHWESTERN SAUDI ARABIA USING LANDSAT-MULTISPECTRAL TECHNIQUES

H. W. Blodget
NASA Goddard Space Flight Center, Greenbelt, Md.

G. F. Brown
U.S. Geological Survey, Reston, Va.

J. G. Moik
Computer Sciences Corp., Silver Spring, Md.

ABSTRACT

Various computer enhancement and data extraction systems using LANDSAT data have been assessed and used to complement a continuing geologic mapping program. Interactive digital classification techniques using both the parallelepiped and maximum-likelihood statistical approaches achieve very limited success in areas of highly dissected terrain. Computer enhanced imagery developed by color compositing stretched MSS ratio data has been constructed for a test site in northwestern Saudi Arabia. Initial results indicate that several igneous and sedimentary rock-types can be discriminated.

CONTENTS

ILLUSTRATIONS

ILLUSTRATIONS (Continued)

GEOLOGICAL MAPPING IN NORTHWESTERN SAUDI ARABIA
USINC LANDSAT-MULTISPECTRAL TECHNIQUES

INTRODUCTION

During the past 25 years, the Saudi Arabian Ministry of Petroleum and Mineral Resources, in cooperation with the U.S. Geological Survey, has actively engaged in the geologic mapping of the Precambrian areas of the Arabian Peninsula. Initial field mapping efforts have contributed to the publication of preliminary geologic maps at 1:500,000 and 1:2,000,000 (U.S. Geological Survey, 1963) scale for the entire peninsula, as well as a tectonic map at 1:4,000,000 (Brown, 1972).

Present geologic goals include mapping the entire shield at 1:100,000 scale. The first few maps in this series have been published during the past several years, but a monumental task is still required to complete this ambitious project.

Various approaches using LANDSAT data are currently being assessed and used to complement the continuing mapping program in this 600,000 km² area. The capability of discrimination of some of the lithologic units appears to be particularly promising.

Figure 1 is a reduction made from a 1:1,000,000 mosaic constructed from 137 LANDSAT frames. The entire Arabian shield is included in this regional coverage, and the approximate margins of the Precambrian outcrop are delineated by the solid black lines. The basement rocks, in general, are seen as varying shades of dark gray. The very dark areas, on the other hand, are most commonly the poorly reflective flood basalts of Tertiary or younger age. The flow identified on the figure provides an example of this poorly reflective rock class. The Precambrian outcrops extend approximately 2000 kilometers from the Gulf of Aqaba on the north, southward to the Gulf of Aden, and attain a maximum width of 700 kilometers, at approximately 23 degrees north latitude.

Figure 2, an enlargement of the northern section of the mosaic, includes the present area of interest. The outlined test site area is located just east of the Red Sea coast in northwestern Saudi Arabia.

Only limited and very generalized rock type distinctions are possible based only on photo interpretation of the various LANDSAT photographic formats. Several very generalized lithologic groupings can be distinguished on the basis of tonal, textural and distribution characteristics. These include: (1) highly reflective alluvium and aeolian deposits, (2) poorly reflective, extensive basalt extrusions, (3) regionally homogeneous sedimentary strata and (4) coarse textured (at
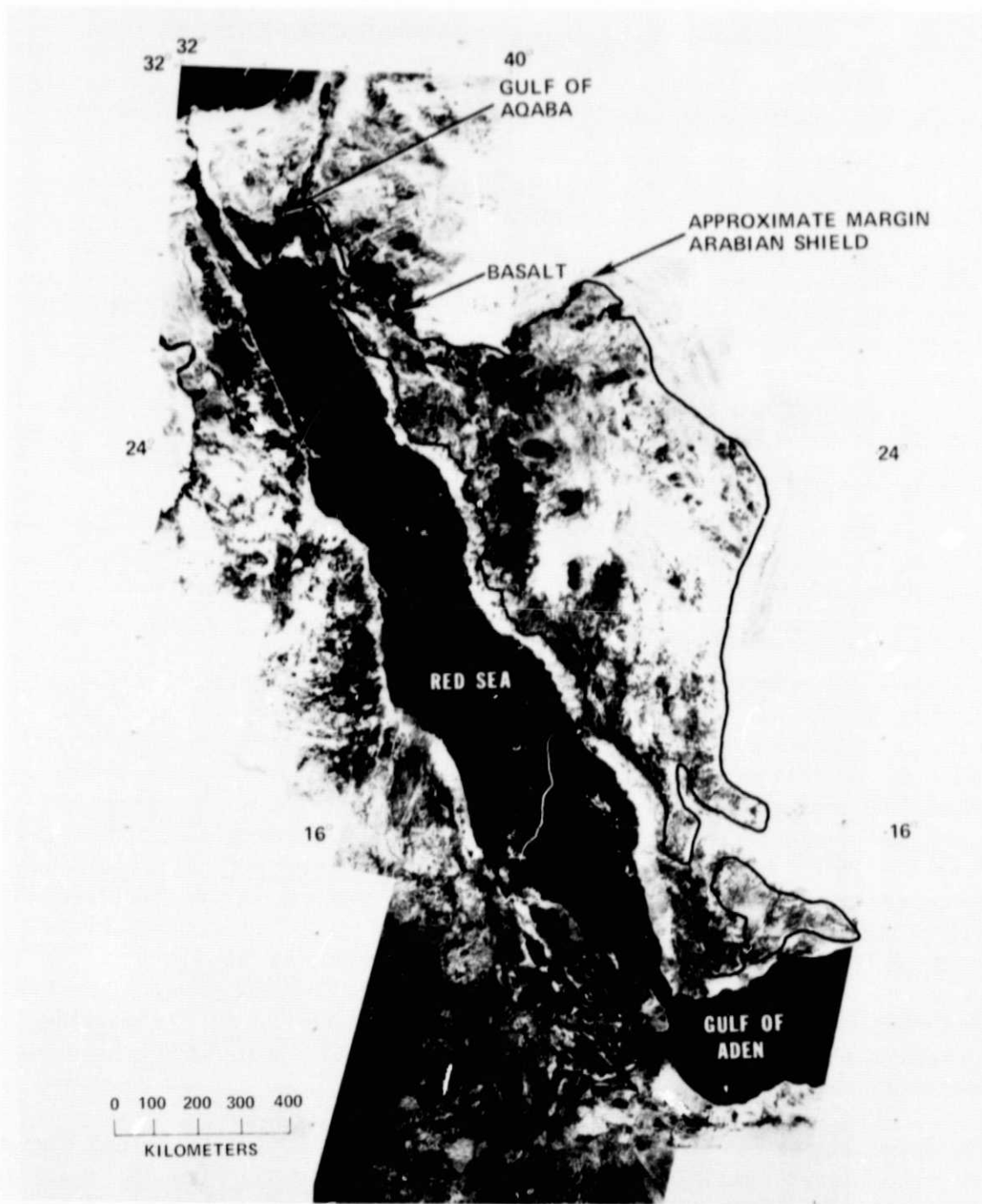
1

Figure 1. Semi-controlled mosaic of the Red Sea and adjacent Precambrian basement. Original constructed from 137 LANDSAT scenes.
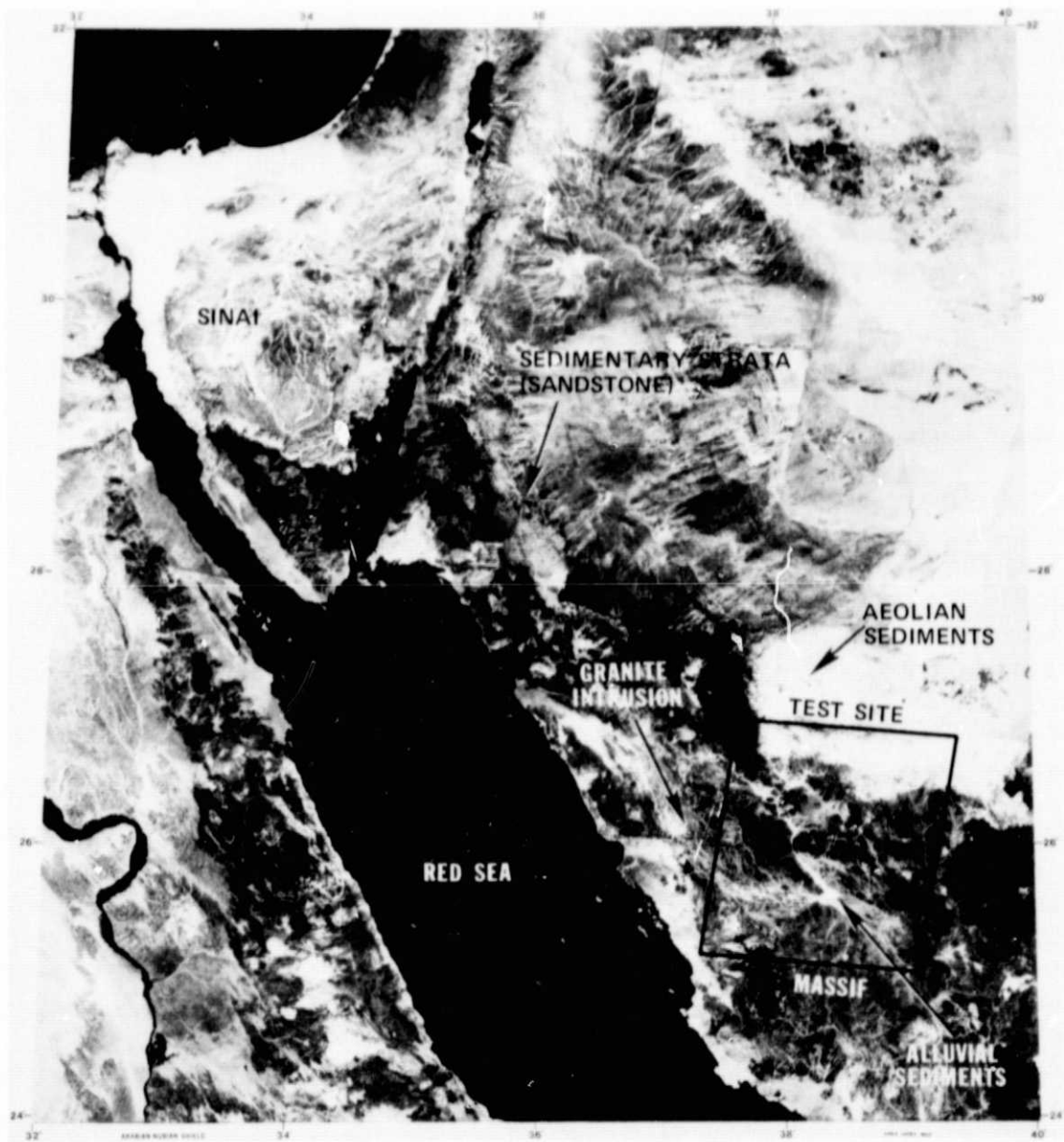
Figure 2. LANDSAT-1 mosaic of northern Red Sea
and adjacent terrestrial areas.

LANDSAT scale) massifs. Within the latter unit, sub-circular, highly reflective intrusions are common in the Red Sea area, and these, where maps are available, are generally designated as being of granitic composition. The high spectral reflectivity associated with these intrusions does not generally appear to be directly related to their discrete mineralogic composition, but rather is an indirect indication of their topographic expression. Using the limited side-lap stereographic coverage available on LANDSAT imagery, light areas associated with these rocks are shown to be topographically low. This would suggest that the intrusions are subject to more rapid mechanical weathering than their respective host rocks. The topographic depressions caused by such differential weathering appear now to be partially filled with highly reflective aeolian and/or alluvial sediments.

Identification of generalized rock-types such as those discussed above, however, are not generally adequate for most geologic mapping objectives. To improve on this discrimination capability, the use of LANDSAT digital data was evaluated using various computer enhancement techniques.

The frame selected for the initial test site (1159-07272) is shown in Figure 3. This particular scene was selected because it includes two of the published 1:100,000 geologic map areas. Thus larger scale geological mapping is available to provide interim "ground truth" for about 20 percent of the scene outlined. Figure 4 includes those portions of the 1:500,000 published geologic maps of the northwestern Hijaz (Brown, Jackson, et al., 1963) and northeastern Hijaz (Brown, Layne, et al., 1963) which correspond to the test site. The slight shape varience of these identical geographic areas is caused by differences in image and cartigraphic projection.

The geology included in the scene consists predominantly of complex Precambrian metamorphic assemblages intruded by plutonic rocks varying in composition from gabbro to granite. On the north, the Precambrian is overlain by northeasterly-dipping sandstone of Cambrian ($\text{\euro}$s) age. Quaternary/Tertiary flood basalts (QTb) make up the dark, less dissected areas in the west and southeast. Several small volcanic flows extend northward at the left side of the bottom margin. Because of the generally low spectral reflectivity and poor tonal contrast, individual igneous and metamorphic units are difficult to distinguish in standard image formats.

Figure 5 is a reproduction of the 1:100,000 Sahl al Matran (Hadley, 1973) map, which is entirely within the test site. The area included is shown in both Figures 3 and 4. The additional detail provided by the larger scale is, of course, immediately recognized. In particular, it should be noted that the generalized granite units (gr) shown at 1:500,000 scale, have been divided and mapped as granite/granodiorite (ggd) on the south, and as two hornblende biotite quartz monzonites intrusions (hbqm) on the north. These units will subsequently be discussed in some detail.

4

APPROACH

In order to determine the applicability of computer classification and/or image enhancement for rock identification in this test area, the several programs available at the Goddard Space Flight Center were assessed. These included interactive, multispectral classification systems, employing both the maximum likelihood and parallelepiped classification techniques and digital image enhancement using the SMIPS-VICAR System* (Moik, 1973). None of the systems have been exhaustively evaluated, but several preliminary conclusions can be projected.

COMPUTER CLASSIFICATION

Based on our preliminary studies of lithology discrimination within the test site, using interactive digital classification techniques, the more successful results were attained with the maximum likelihood approach incorporated into the Bendix M-DAS system. The most positive results attained with this system are shown on Figure 6.

Training sites were selected for ten lithology classes, which fell into three general categories. These included: (1) Rocks mapped at 1:100,000 scale which did not appear distinctive in the color composite imagery. In this category, training sites were selected within the Halaban group (hjm) and older greenstones (gd) mapped near the base of the Sahl al Matran Quadrangle in order to determine if these units could be separated on the basis of their spectral differences. (2) Rocks somewhat distinctive on the composite imagery that correspond with field mapped units. These units included flood basalts (QTb) mapped on the Northwest Hijaj Quadrangle and a granite/granodiorite (ggd) mapped at 1:100,000 on the Sahl al Matran Quadrangle. (3) Sediment units that appear to be distinctive on the composite imagery but have not been subdivided on the 1:100,000 geologic maps. The six training sites selected in this category were established in alluvium having different tonal characteristics on standard LANDSAT imagery. In some cases, it appears that discrete alluvial units can be in part related to their specific source rocks.

Clearly, the units defined in red (basalt),**purple, yellow and dark blue (tonal alluvial units), correlate best with the geologic maps and the original MSS imagery. The granite/granodiorite (ggd) though not uniquely distinctive, does appear to be off-white, and its related alluvium depicted in dark blue, defines the general outcrop area mapped on Figure 5.

---

*Small Interactive Image Processing System, an interactive version of the Jet Propulsion Laboratory VICAR System.

**All color descriptions in this text are based on original color imagery. Tonal changes are generally visible on the equivalent black-white figure format but these are considerably less definitive.

Figure 3. Northwestern Saudi Arabia test site. Areas included on Sahl al Matran (Hadley, 1973) and Wayban (Hadley, 1974) 1:100,000 geologic maps are indicated by the northwest and southeast insets respectively.

6
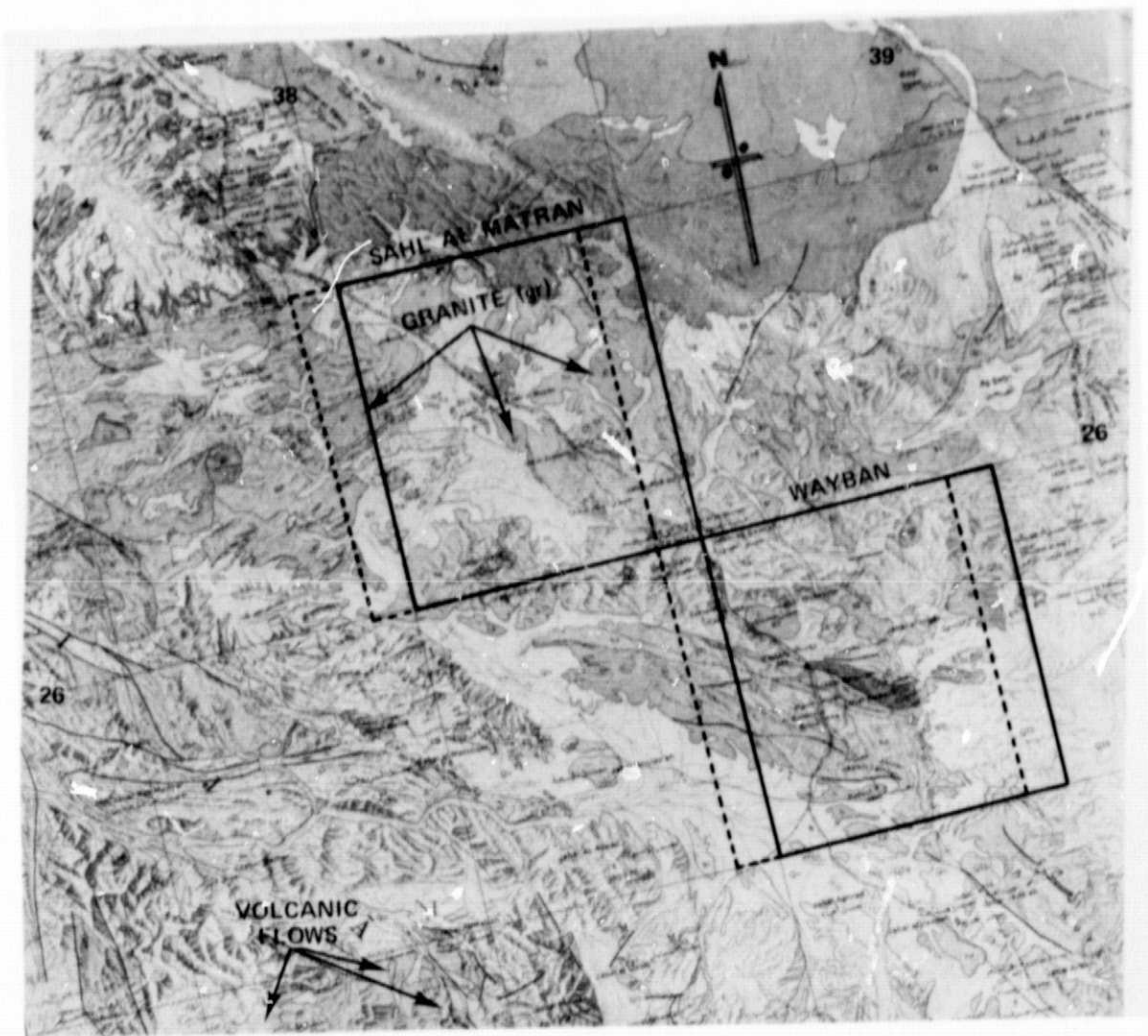
Figure 4. Northwest Saudi Arabia test site geological map, modified after Brown, Jackson, et al. (1963) and Brown, Layne, et al. (1963). Original at 1:500,000 scale. Areas of published 1:100,000 geologic map coverage outlined. Note revised longitude shift to west on larger scale maps.
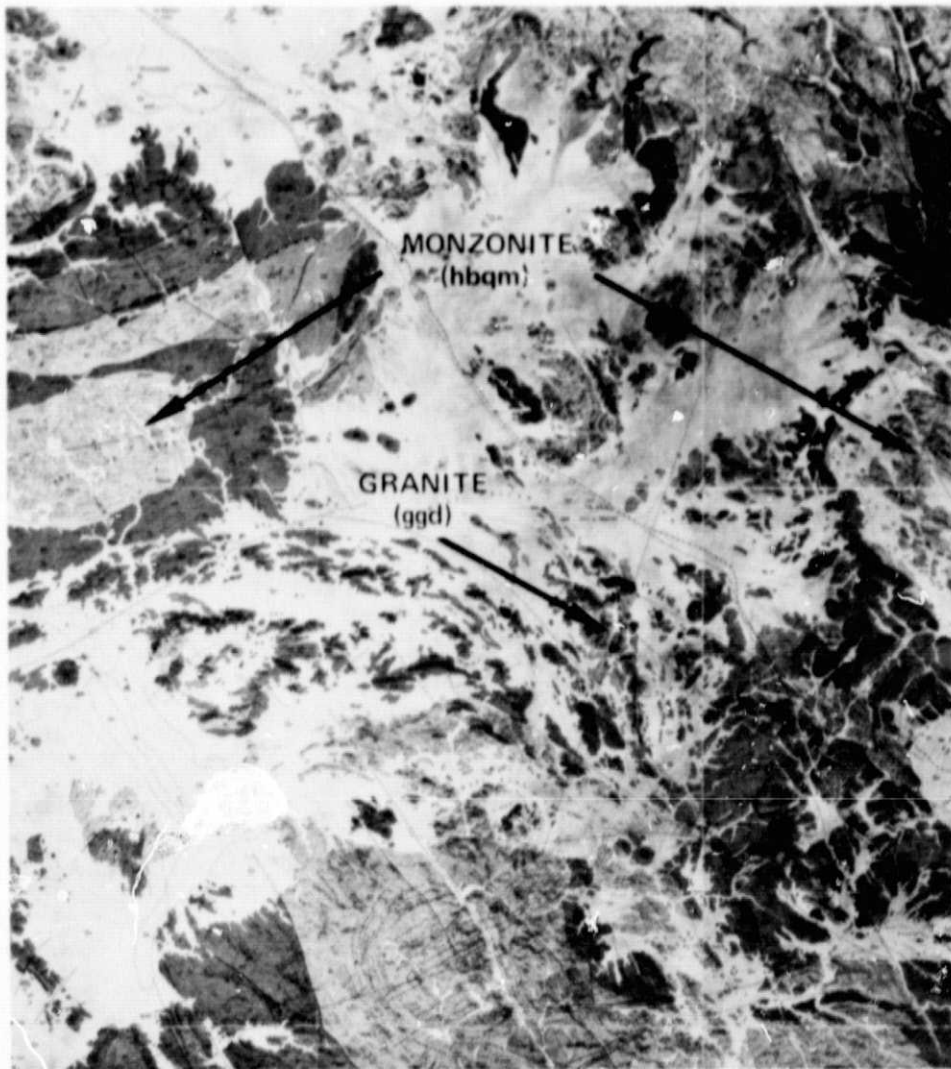
Figure 5. Geologic map of Sahl al Matran quadrangle,
after Hadley (1973). Original at 1:100,000 scale.

On the other hand, no obvious discrimination can be made in the highly dissected
metamorphic and igneous terrains. It is important to note here that the more
consistently correct classification is associated with the most homogeneous,
near-horizontal beds formed by the flood basalts (red) and alluvium (purple, yel-
low and dark blue).

Figures 7 and 8 are computer enlargements of portions of the basalt and granite/
granodiorite classes defined in Figure 6. The small boxes within each unit desig-
nate the training sites selected for classification. In both figures, the generally

8

Figure 6. Classification of part of the northwest Saudi Arabia test site using the maximum likelihood approach. Enlarged areas shown on Figures 7 and 8 are outlined. Note: Text based on original color imagery. Grey tonal changes are less definitive.

9

Figure 7. Computer enlargement of basalt (QTb) class using maximum-likelihood classification. Angular box is training site for this class. Note: Text based on original color imagery. Grey tonal changes are less definitive.

10

Figure 8. Computer enlargement of granite (ggd) class using maximum-likelihood classification. Rectangular box is training site for this class. Note: Text based on original color imagery. Grey tonal changes are less definitive.

11

poor definition of the class-unit margins is emphasized when compared with the equivalent mapped formations shown on Figures 4 and 5 respectively.

Based on our preliminary assessment of classification systems in this test site, it is concluded that the multispectral classification techniques appear to be severely limited for lithology mapping. One prime reason for this is the extreme difficulty encountered in defining adequate training sites in areas of highly dissected terrain.

COMPUTER ENHANCEMENT

Of the various rock discrimination approaches tested to date, a technique using color composites constructed from enhanced ratio data has proven to be most successful at this particular test site. An excellent summary of this method is provided by Rowan, et al. (1974).

In simplified form, the procedure consists of three fundamental steps: (1) Selected MSS bands are ratioed pixel by pixel, (2) the ratio data are stretched to enhance contrast and converted into black-white positive film imagery and (3) the stretched images of three ratio combinations are combined into color composite imagery using various combinations of light filters and intensities.

In the ratioing procedure, alternative ratio combinations are used to enhance specific rock classes. The 4/5, 5/6, and 6/7 combinations have provided the greatest single discrimination capability for both the Saudi Arabia test site and the Nevada test site of Rowan. In the Sahl al Matran area, however, other ratio combinations have successfully provided identification of additional rock classes. Optimum ratio combinations are often found to be scene dependent, and at present, no general rule exists for selecting the best combinations to provide the greatest discrimination capability over a wide range of climatic, topographic and/or lighting conditions. Goetz and associates (Goetz, 1975, Goetz and Rowan, 1975) are conducting field studies using a portable field reflectance spectrometer to better define the optimum spectral and ratio combinations for specific applications.

Both linear and nonlinear stretch processes can be alternatively used to optimally increase scene contrast over the dynamic range of the output product. Linear stretching increases the scene contrast uniformly over the dynamic range while nonlinear stretching is used to increase local scene contrast in parts of the intensity range at the expense of other portions of the spectral range. In our test area, histogram equalization provided maximum intrascene contrast. Here again, as with the selection of ratio combinations, there are presently no general rules that can be applied to all images to determine the optimum stretch parameters for a given set of conditions.

12

We have been using a rotating drum film recorder (OPTRONICS) to construct black and white photo transparencies from the digital images. The various combinations thus constructed are then combined in a color-additive viewer to rapidly determine the more significant combinations in regard to rock discrimination capability. Once these combinations are defined, they are processed through a CRT film recorder (DICOMED) to produce hard copy with a better registration than that attained on the color-additive viewer.

The resultant composite provides the distinct advantage of displaying a single type of material as being similar or the same regardless of the local variation due to albedo and topography. Conversely, however, very dissimilar materials easily separable on a standard composite image may become inseparable on a ratio image where spectral reflectively slopes are similar. Thus, optimum rock-type discrimination must be accomplished in several combinations of different ratio combinations.

All digital enhancements described in this study were performed using an interactive image processing system on IBM/360-75 or -91 computers.

Figure 9 is a DICOMED ratio-composite where the MSS band 4/5 ratio image is projected with a blue filter, 5/6 image with a green filter, and 6/7 image with a red filter. Note in this presentation that the monzonites (hbqm) mapped on the Sahl al Matran Quadrangle are a dark green while the granite/ granodiorite (ggd) and alluvium around the granites are ocher in hue. Outside the Matran map area, at the right margin, a dark green triangular body has also been mapped as a hornblende-biotite quartz monzonite on the 1:100,000 Wayban Quadrangle (Hadley, 1974). In addition the ocher-brown body immediately to the west of the monzonite is mapped as riebeckite granite (rg). There is no 1:100,000 coverage of the ocher-colored area to the north, but it is also shown as granite (gr) on the 1:500,000 Northwestern Hijaz Quadrangle.

The brilliant blue* unit on the composite, of course, corresponds to the basalt flow (QTb) classified on Figure 6. It can be seen very clearly here that the margins of the basalt are much more distinctly defined than they were using a computer classification system (Fig. 7). In addition to these flood basalts, several smaller flows are seen near the eastern margin of the image and several discrete cinder cone fields are visible across the wadi from the large flow. This enhancement has been used to aid in distinguishing small cinder cones of basaltic composition from ultramafic rocks in the preliminary 1:100,000 map compilation for the area south of the Sahl al Matran Quadrangle.

---

*Blue reproduces as light grey in the black-white format and therefore it is difficult to distinguish basalt from the underlying schist in Figure 9. Please refer to Figures 11 and 12 for better definition of these flows.
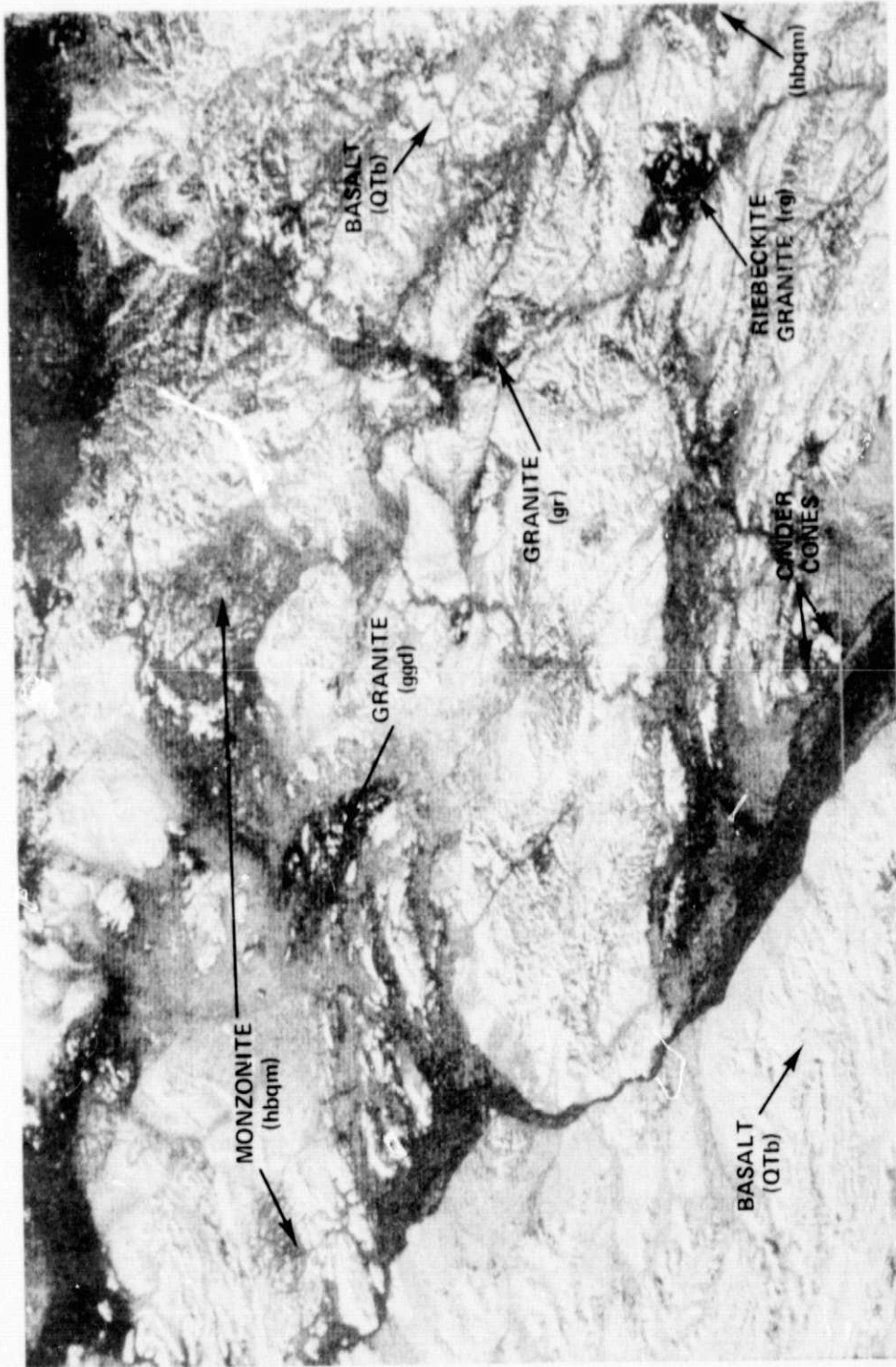
13

Figure 9. DICOMED ratio-composite of a part of the northwest Saudi Arabia test site. Constructed from MSS 4/5 ratio imagery projected through a blue filter, MSS 5/6 imagery through a green filter and MSS 6/7 imagery through a red filter. Note: Text based on original color imagery. Grey tonal changes are less definitive. Refer to Figures 11 and 12 for better definition of basalt.

14

The tan-colored outcrops in this enhancement are mostly complex metamorphic assemblages. Our ability to distinguish between metamorphic units mapped in the field has been poor to date.

Figures 10 and 11 were photographed from a color additive viewer screen. Some resolution degradation caused by the poor registration of the different ratio images results in a slight blurring. The points of reference, however, can still be readily distinguished.

The Figure 10 image was made from a combination using MSS band ratio 4/7 imagery with blue filter, 7/4 imagery with a green filter, and 6/5 imagery with a red filter. In this rendition, the Siq sandstone (€s) in the upper right, is a bright yellow. This is not unique to the scene, however, for granites (gr) to the south are of the same hue. It is thus not possible to distinguish between the two different lithologic units on the basis of this particular ratio enhancement alone. When the MSS 6/5 band ratio image is replaced by 7/6 image using a red filter, however, tonal changes occur as shown in Figure 11. In this second ratio composite, the Siq sandstone remains a bright yellow, but the granites that were yellow in Figure 10 are now a pale yellow-green hue. Conversly, the monzonite (hbqm), that is pale yellow-green in Figure 10, is now yellow on Figure 11 with the new ratio combination. The use of a pair of ratio combinations, thus, seems adequate in this case to define the Siq sandstone within this particular scene; at the same time, the inherent spectral characteristic differences between granites and monzonites are reemphasized.

Figure 12 is a DICOMED ratio-enhancement that overlaps the area shown in Figure 9, on the south. This color ratio-composite was made using MSS 5/4 imagery with a blue filter, 6/5 imagery with a green filter, and 7/6 imagery with red filter, or just the inverted ratio combinations used in the construction of Figure 9. The several volcanic flows that extend northward from the left side of the bottom margin of the test site (Fig. 3) are shown in two colors in this ratio-enhancement. Based on field confirmation, the geologically recent flows correlate with the areas shown in ocher while the flows of historic age are shown as black (the most recent eruptions in the area were recorded in 1280 A. D.). The flood basalts (QTb) that were blue in Figure 9 are a bright yellow in Figure 12. There is, thus, a strong suggestion that the progression of color tonal differences from black to ocher to yellow among the basalts can be at least crudely related to age. Fundamental differences in chemical composition of the respective flows could provide an explanation for the color differences. Field data, however, suggest that the compositional differences are not sufficient to significantly alter the spectral response between the different volcanic units. Changes in reflectance due to a varying degree of weathering, on the other hand, better explain the observed difference of spectral response, and of course, this would also relate to age differences.

15

Figure 10. Ratio-composite enhancement photographed from a color additive viewer screen. Composite is constructed from the MSS 4/7 ratio image projected through a blue filter, the MSS 7/4 image through a green filter and MSS the 6/5 image through a r filter. Note: Text based on original color imagery. Grey tonal changes are less definitive.

16

Figure 11. Ratio-composite enhancement photographed from a color-additive viewer screen. Composite is constructed from MSS 4/7 ratio imagery projected through a blue filter, MSS 7/4 imagery through a green filter and MSS 7/6 imagery through a red filter. Note: Text based on original color imagery. Grey tonal changes are less definitive.

Figure 12. DICOMED ratio-composite of a part of the northwest Saudi Arabia test site. Constructed from MSS 5/4 ratio imagery projected through a blue filter, MSS 6/5 imagery projected through a green filter and MSS 7/6 imagery through a red filter. Note: Text based on original color imagery. Grey tonal changes are less definitive.

18

In addition to the mapped extrusives discussed above, there appears to be a distinct lithologic class defined in pale yellow in the southeast corner of Figure 12. The entire lithologic suite in this quadrant has been mapped as schist (sc) at small scale (see Fig. 4). The enhanced imagery was compared with a 1:100,000 orthophoto mosaic of the area which had been constructed from reduced 1:30,000 aircraft photography, and it was found that the pale-yellow spectral unit defined on the ratio-enhanced image correlated extremely well with a clearly defined, dark, "botryoidal"-textured unit on the mosaic. It is anticipated that this unit will be investigated in the field to determine if the pale-yellow unit does indeed define a specific metavolcanic sequence.

Most of the western one-fourth of Figure 12 is within the area to be included in the 1:100,000 Dhaylan Quadrangle. The lithology change across the well-defined north-south trending fault (A-A') is especially well displayed on the south where an abrupt color change occurs from purple on the west to a dark-brownish-green on the east. The southern part of the pale green sinuous body (gr) is designated as granite on the preliminary geologic map. On the same map, however, this granite is shown to terminate at a secondary fault extending between B and B' on Figure 12. The ratio composite data, however, strongly suggest that the granite continues in a northwesterly direction as a discrete unit, and terminates at the major north-south fault. This area must be further investigated in the field to determine the true extent of the granite body.

To complement the spectral-lithologic relationships discussed above, special attention was placed on the areas immediately adjacent to the three ancient mine workings described by Hadley (1972). Each area was studied in detail using a variety of ratio/filter and stretch combinations in order to identify any hydrothermal alteration that might be associated with the mineralization. No anomalies were recognized, but this could very well be due either to the absence of alteration products or the small areal extent of mineralized areas. Plans are presently being formulated to study several well-developed hydrothermal alteration zones known to exist in association with the massive Wadi Wassat sulfide deposits near the Yemen border.

CONCLUSIONS

The ability to identify lithologic classes using LANDSAT multispectral techniques appears to be possible, at least to a limited degree. The various classification techniques that have been so successful in a variety of agriculture, land use and environmental studies appear to be severely limited in rock-type discrimination, especially in areas of highly dissected terrain. This is not necessarily the result of the inadequacy of the various statistical approaches used in classification, but rather, the extreme difficulty encountered in defining adequate training sites in areas of highly dissected terrain.

19

A technique of image enhancement using stretched ratio-composite data uses slope difference as the basis for discrimination rather than absolute reflectance values. By using this approach, spectral differences caused by the effects of local variation of terrain and albedo are minimized.

Preliminary studies, using images constructed using this technique, indicate that several rock-types can be distinguished. These include basaltr, monzonites, and certain granites. Efforts to distinguish between different metamorphic lithologies have been unsuccessful.

Computer enhanced LANDSAT imagery continues to be used in selected test sites to complement traditional mapping techniques in Saudi Arabia. The initial promising work is being refined and expanded to form a base from which we can expand and refine our present capabilities.

REFERENCES

Brown, G. F., 1972, Tectonic map of the Arabian Peninsula: Ministry of Petroleum and Mineral Affairs map AP-2.

Brown, G. F., Jackson, R. O., Bogue, R. G., and Elberg, E. L., Jr., 1963, Geologic map of the northwestern Hijaz Quadrangle, Kingdom of Saudi Arabia: U.S. Geological Survey Misc. Geol. Inv. map I-204A.

Brown, G. F., Layne, N., Goudzarzi, G. H., and MacLean, W. H., 1963, Geologic map of the northeastern Hijaz Quadrangle, Kingdon of Saudi Arabia: U.S. Geological Survey Misc. Geol. Inv. map I-205A.

Goetz, A. F. H., 1975, Use of ERTS and other correlative data: in Goetz, A. F. H., Billingsley, F. C., Gillespie, A. R., Abrams, M. J., Squires, R. L., Shoemaker, E. M., Lucchitta, I. and Elston, Application of ERTS images and image processing to regional geologic problems and geologic mapping in northern Arizona; Jep Propulsion Laboratory, California Institute of Technology Technical Report 32-1597, p. 4-12.

Goetz, A. F. H., and Rowan, L. C., 1975, The realities of using satellite spectral data for lithologic identification: Presented at Annual Mtg. of the Am. Soc. of Photogrammetry, Washington, D.C., March 9-14.

Hadley, D. G., 1973, Geology of the Sahl al Matran Quadrangle, northwestern Hijaz, Kingdom of Saudi Arabia: Ministry of Petroleum and Mineral Resources map GM-6.

Hadley, D. G., 1974, Geologic map of the Wayban Quadrangle, Kindom of Saudi Arabia: Ministry of Petroleum and Mineral Resources map GM-7.

Moik, J. G., 1973, Small interactive Image Processing System, User's Manual: NASA/GSFC X-650-73-283, 61 p.

Rowan, L. C., Wetlaufer, Goetz, A. F. H., Billingsley, F. C., and Stewart, J. H., 1974, Discrimination of rock types and altered areas in Nevada by use of ERTS images: U.S. Geol. Prof. paper 883, 35 p.

U.S. Geological Survey-Arabian American Oil Company, 1963, Geologic Map of the Arabian Peninsula: U.S. Geological Survey Misc. Geol. Inv. map I-270A.